Available at: http://publications.ictp.it IC/2010/100

United Nations Educational, Scientific and Cultural Organization
and
International Atomic Energy Agency
THE ABDUS SALAM INTERNATIONAL CENTRE FOR THEORETICAL PHYSICS

ELECTRON AND HOLE STATES IN STAINED InAs/GaAs QUANTUM DOTS: SIZE AND MAGNETIC FIELD EFFECTS

K. Sellami[1]
Laboratoire de Physique des Materiaux, Faculté des Sciences de Bizerte,
Universite 7 Novembre à Carthage, 7021 Jarzouna, Tunisia
and
The Abdus Salam International Centre for Theoretical Physics, Trieste, Italy,

I. Saïdi, M. Yahiaoui
Laboratoire de Physique des Materiaux, Faculté des Sciences de Bizerte,
Universite 7 Novembre à Carthage, 7021 Jarzouna, Tunisia,

C. Testelin
Institut des Nanosciences de Paris, Universites Paris VI et VII, CNRS-UMR 7588,
Campus Boucicaut, 140 Rue de Lourmel, 75015, Paris, France

and

K. Boujdaria
Laboratoire de Physique des Materiaux, Faculté des Sciences de Bizerte,
Universite 7 Novembre à Carthage, 7021 Jarzouna, Tunisia.

MIRAMARE – TRIESTE
December 2010

[1] Corresponding author: karimsellami@yahoo.fr

Abstract

A method for the calculation of the electronic structure of truncated-cone self-assemled InAs/GaAs quantum dots is presented. The method is based on using a 40-band k.p model to calculate the band structure of strained InAs/GaAs quantum dots, and extract the different band parameters for the calculation of the electronic properties of the InAs/GaAs quantum dots. Then, using an exact numerical matrix diagonalization technique, we calculated numerically the electron and hole eigen energies and associated eigen states. We considered thereafter the effect of an external applied magnetic field, strain and quantum dot size variation on the charge carrier energy levels. It is clearly found that the strain strongly modifies the quantum dot potential profile, leading to a different electron and hole energy distribution. Our results revealed also that the electron and hole energy spectra change significantly when varying the quantum dot size as well as the magnetic field. Given this striking nanostructure size and magnetic field energy dependent property, these systems provide the opportunity to control and tune their optical and electronic properties through these parameters, which is important in order to optimally tailor optoelectronic devices based on quantum dots.

I. INTRODUCTION

Semiconductor (SC) quantum dots (QDs) continue to receive a great deal of attention, largely due to their unique properties arising from δ-function like profile of the density of states, in view of both the high potential for applications as well as new physics on a nanoscale [1–4]. The basic understanding of the quantum dot (QD) properties is necessary in order to fully exploit their application potential. Several methods for fabrication of QDs have been reported over the last decade including lithography-based technologies. Although this technique is widely used to provide QD predominantly by the combination of high-resolution electron beam lithography and etching, the spatial resolution required for reaching the size regime where significant quantization effects can be expected tends to be larger than the desirable level. In addition, lithographic methods and subsequent processings often produce contamination, defect formation, size non-uniformity, poor interface quality, and even damage to the bulk crystal itself [5, 6]. The most effective and valuable method for the fabrication of coherent, dislocation-free 10 nm semiconductor QDs is the strained-layer epitaxy in the Stranski–Krastanow mode [7, 8]. Such self-organized transformation from two-dimensional layer-by-layer growth, traditionally called the wetting layer, to a three-dimensional mode was found for many heterostructure systems. As one of the most prominent realizations of these three-dimensional carrier confinements, self assembled InAs (or $In_xGa_{1-x}As$) QDs have been studied in great detail [9]. Single InAs QDs in GaAs matrix represent the best studied model system, and have attracted escalating interest due to their suitability as the basis for photon emission technology for applications in quantum information [10]. Indeed, the discrete energy states and the ease of integration into an optoelectronic device recently lead, e.g., to the presentation of electrically driven single photon sources [8]. The engineering of strain-induced self-organized SC QDs relies on a mismatch between lattice constants of the dot material and the substrate on which the dots are grown. The ensuing strain inside the QDs can be significantly larger than in ordinary (i.e., flat, parallel interfaces) SC heterostructures because in the latter case large strains must be avoided to prevent dislocations (mismatch $\leq 2\%$), whereas in nonflat geometries of InAs QDs grown on GaAs the mismatch 7% can even be tolerated. As a consequence of this great lattice mismatch, large strains are present in the structure and strongly modify the potential profile along the growth axis. This strain plays an important role in the growth of these SC heterostructure, and it is essentially important to probe strain in these system. Consequently the accurate modelling of its profile is an essential prerequisite for electronic structure calculations, and also for the clear understanding of the growth of self-assembled QDs. In order to enhance optoelectronic device performance, one must be able to control the size, shape and distribution of the QDs leading also to a better knowledge of the electronic structure of these nanostructures which is essential to understand their physical properties. For instance, in a recent work, Campbell-Ricketts et *al* [11] have pointed out the important role of the dot height in determining exciton lifetimes in shallow InAs/GaAs QDs. C.Y. Ngo et *al* [12] reported

also that the size and shape exert a significant influence on the InAs/GaAs QD electronic states. The effects of an applied magnetic field on the physical properties of QDs have been studied with interest from the theoretical and experimental points of view. These studies have been performed with the proposal of understanding the fascinating novel phenomena and of fabricating devices with new functions or to improve the performance of the existing devices [13]. It turned out also that the application of a very large magnetic field can give important insight into this problem. Although the application of a magnetic field has proven to be a very powerful tool for studying the optical and electronic properties of SC materials, the magneto-optical study of self assembled QDs requires the application of very strong magnetic fields, in the order of tens of Tesla, in order to provide anything more than a small perturbation to the orbital motion of strongly confined carriers [14].

In this work we report theoretical study of the strained InAs/GaAs self assembled QD under an applied external magnetic field. This paper is organized as follow : Section II presents the calculation of the strained dot material energy band structure and band parameters. These calculations were performed using an accurate 40-band **k.p** and Bir-Pikus hamiltoninan model. In Sec. III we give, within the frame work of the effective mass approximation, the electron and hole hamiltonian under an applied magnetic field, considering a cylindrically symmetric truncated cone shaped QD lying on a wetting layer. We computed the electron and hole eigen states using a numerical diagonalization approach. In a next step we investigated theoretically the effect of the size and magnetic field variation on the charge carriers energy in the QD. The Sec. IV is devoted to the conclusion.

II. ENERGY BAND STRUCTURE AND BAND PARAMETERS IN STRAINED InAs

Epitaxially grown SC structures often consist of materials with different lattice constants. The mismatch of lattice constants creates strain fields in QD heterostructures, which affect the optoelectronic properties of QDs. Hence the knowledge of strained SC band structure is of prime importance in particular for InAs/GaAs QD where an accurate modeling requires the complete dispersion relation of the electrons and holes in strained InAs. In order to solve the electronic Schrödinger equation in strained InAs on GaAs with a biaxial [001] strain, we use the total Hamiltonian $H = H_{\mathbf{kp}} + H_s$, where $H_{\mathbf{kp}}$ is a 40-band **k.p** Hamiltonian and H_s is the strain Bir-Pikus Hamiltonian.

In a recent article [15], we have developed the 40-band **k.p** model in order to calculate the band parameters of several zinc-blende-type SCs. The role of the d-type valence bands (VBs) in the calculation of the band structure of bulk SCs is considered in Ref.15. We have reported that $H_{\mathbf{kp}}$ Hamiltonian allows one to compute the fundamental parameters such as Luttinger parameters, the κ VB parameter, the effective g* Landé factor, the effective masses, and the δ Dresselhauss [or bulk inversion asymmetry (BIA)] spin-orbit coupling constants. We have also reported that

whenever the experimental data are available, our **k.p** calculations agree with them.

We now describe the H_s Bir-Pikus Hamiltonian. As mentioned above, the biaxial [001] strain is due to the difference between the bulk GaAs and the bulk InAs lattice constants. The [001]-strain tensor elements take the form [16]

$$\epsilon_{xx} = \epsilon_{yy} = \epsilon_{\shortparallel} = \frac{a_0(GaAs) - a_0(InAs)}{a_0(InAs)}$$

$$\epsilon_{zz} = \epsilon_{\perp} = -2\frac{C_{12}}{C_{11}}\epsilon_{\shortparallel}$$

$$\epsilon_{xy} = \epsilon_{xz} = \epsilon_{yz} = 0$$

where C_{11} and C_{12} are the elastic stiffness constants. The strain Hamiltonian matrix is well known [17]. It can be obtained from the **k.p** matrix element. It can be easily included by the same summetry consideration and a straightforward addition of corresponding terms $k_\alpha k_\beta \rightarrow \epsilon_{\alpha\beta}$ ($\epsilon_{\alpha\beta}$ have exactly the same symmetry as $k_\alpha k_\beta$) with the deformation potentials a_c, a_v, and b_v at the corresponding positions of $\frac{\gamma_C}{2}$, $-\frac{\gamma_1}{2}$ and $-\gamma_2$. Hence the Bir-Pikus Hamiltonian matrix takes the same form that the ones given in Eq. (3) of Ref. [18]. Because the influence of strain on p-type conduction band is unknown, we have taken the p-type CB hydrostatic deformation potential ($a_{\Gamma_{5c}}$) and the p-type CB shear deformation potential ($b_{\Gamma_{5c}} = 0$) equal to zero. Moreover, we do not use the Bir-Pikus Hamiltonian for the s-type VB, which is at $-12.69eV$ from the top of the VB, because (i) no parameters are available for this band and (ii) its influence on the CB and on the VB of interest is very small. Thus, we consider $a_{\Gamma_{1v}} = 0$. In the same way there is no need to apply the strain to the d-type valence and conduction bands.

The band structure of InAs grown on GaAs calculated following our model is shown in Fig (1). Strain has strong consequences on the band diagram particularly in the VB. It lifts the degeneracy between heavy holes (HH) and light holes (LH) at the center of Brillouin zone. In compressively strained InAs, LH are lowered as compared to HH. However, strain do not split the valleys along the growth direction Δ in the CB. Moreover, all the L valleys remain equivalent. Numerical results concerning the band parameters are given in Table (I). This table shows a typical example of how the strain affects the band parameters in bulk SCs. Figure 2 shows a comparison between bulk InAs density of states (DOS) obtained from different band diagram calculations. The present calculation shows that the DOS provided by the total Hamiltonian $H = H_{\mathbf{kp}} + H_s$ is somewhat different to the DOS only given by $H_{\mathbf{kp}}$ Hamiltonian. In contrast

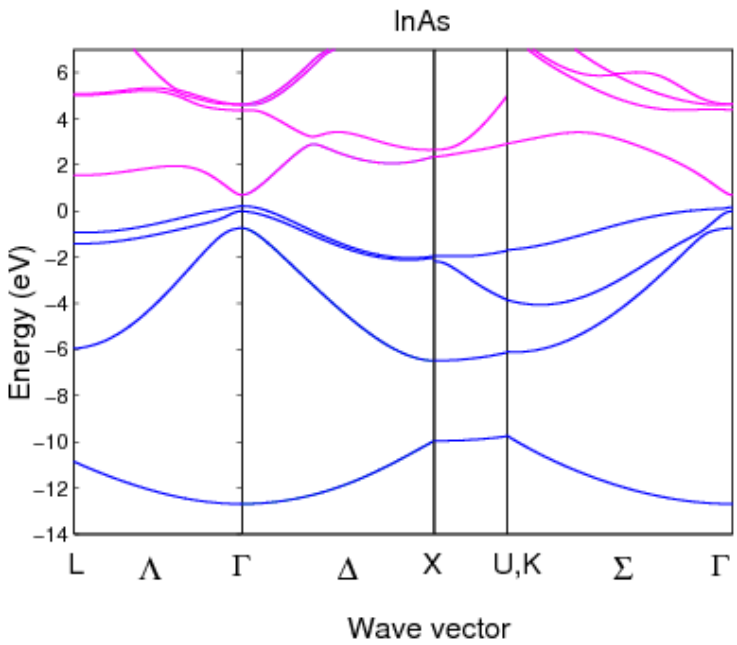

FIG. 1: Energy-band structure in strained InAs obtained with a 40-band **k.p** and Bir-Pikus Hamiltonian model.

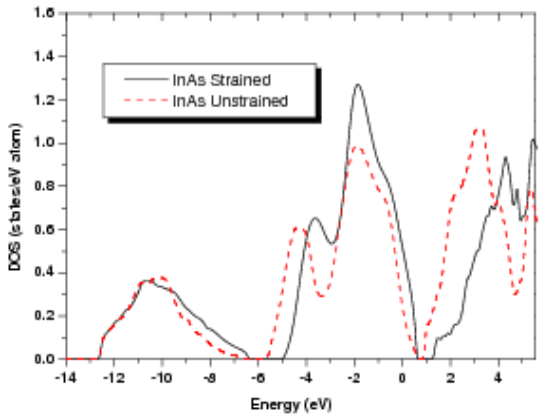

FIG. 2: Density of states (DOS) in the valence band and conduction band for strained InAs grown on GaAs buffer at 0K. The solid-line represents the DOS obtained with the total hamiltonian $H = H_{\mathbf{k.p}} + H_S$ (see the text). The curve in dashed-line is calculated without taking into account the strain effects.

to the common $H_{\mathbf{kp}}$ Hamiltonian, our total Hamiltonian H contain not only information about $H_{\mathbf{kp}}$ but also have distinct information about the behaviour of strain on the DOS. In Fig 2, the curve in solid-line describes the influence of the strain on the DOS and clearly shows that the strain affects the DOS not only in the VB but also in the CB.

a_0	6.057	E_{P3d}	11.11
a_c	-5.40	E_{P2d}	22.41
a_v	0.60	E_{3dV}	0.012
b_v	-1.8	E_{3cV}	0.63
C_{11}	0.833	E'_{PdV}	3.07
C_{12}	0.453	E'_{P3V}	0.92
E_P	17.13	E_{dV}	3.13
E_{PX}	17.97	E_{SdV}	0.01
E_{P3}	4.82	E_{udV}	1.87
E_{P2}	2.51	E'_{P3d}	0.09
E_{PS}	5.23	E'_{P3dV}	0.42
E_{PU}	21.84	E'_{PxdV}	0.77
E_{dd}	1.98	E'_{P2d}	0.06
E'_P	0.11	γ_1	17.69
E_{Pd}	0.48	γ_2	7.42
E_{PXd}	6.34	γ_3	8.23

TABLE I: Numerical values of band parameters used in this work for strained InAs. The lattice parameter a_0 is given in Å. The deformation potentials $a_c$for s-type conduction band and a_v, b_v for p-type valence band are given in eV. C_{11} and C_{12} are the elastic moduli (stiffnesses) given in MPa. The other parameters are calculated to obtain the band diagram given in Figure 1. The related energies $E_{pj}^{(')}$ are given in eV. The γ_j (j=1, 2,3) are the Luttinger parameters.

III. QUANTUM DOT ENERGY LEVELS

A. Formalism

In the framework of the effective mass approximation the electron (hole) Hamiltonian is written as:

$$H = \frac{P_{e(h)}^2}{2m} + V_{conf} + \frac{m_{e(h)}}{2}(\frac{\omega_{ce(h)}}{2})^2\rho^2 - i\frac{\hbar\omega_{ce(h)}}{2}\frac{\partial}{\partial\theta} + g_{e(h)}\mu_B\overrightarrow{B}.\overrightarrow{\sigma}$$

where $m_{e(h)}$ is the electron (hole) mass calculated using the described above 40-band **k.p** model; $\omega_{ce(h)}$ is the electron (hole) cyclotron frequency which is written as function of the magnetic field B applied along the growth direction as: $\omega_{ce(h)} = \frac{eB}{m_{e(h)}}$, and $g_{e(h)}$ is the Landé factor taken from Ref.20. V_{conf} denotes the QD confinement potential that takes into account the shape of the nanostructure chosen as a truncated cone as represented in Fig.3 This potential can be expressed as $V_{conf} = V_0(1 - D(z, \rho))$, where V_0 is the band offset potential calculated also from the energy band structure diagram using the 40-band **k.p** model. The term D in the potential expression is the quantum domain which is written as: $D(z, \rho) = D^{QD}(z, \rho) + D^{WL}(z, \rho)$, where D^{QD} and D^{WL} stands for respectively the quantum and wetting layer domains. These domains are expressed in the following way:

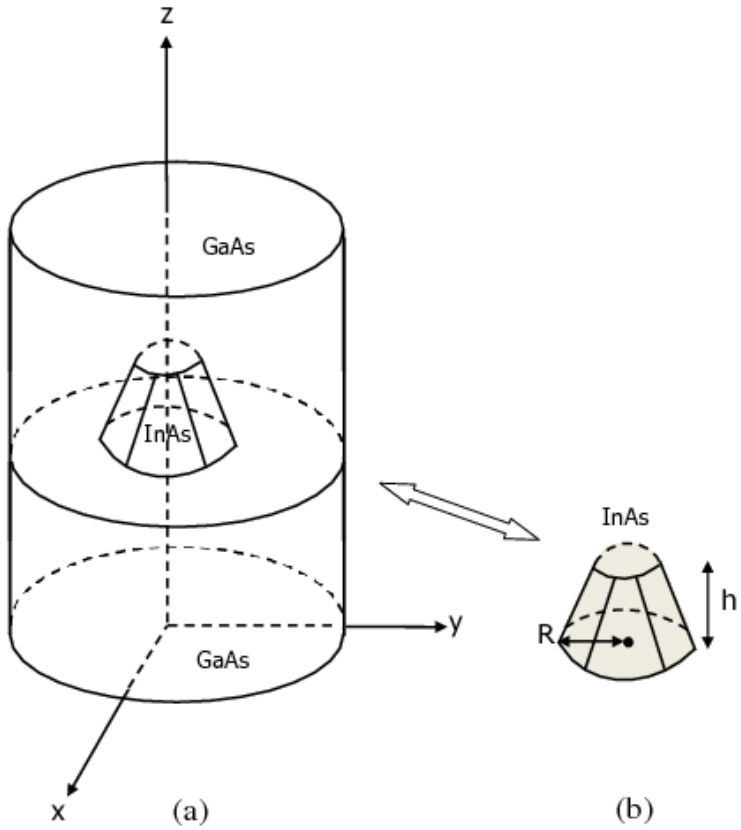

FIG. 3: Geometry of the quantum dot nanostructure. (a) InAs/GaAs heterostructure, and (b) truncated cone shaped InAs quantum dot island, where R represents the QD radius and h its height.

$$\begin{cases} D^{WL}(z,\rho) = \Theta(z)\Theta(d-z) \\ D^{QD}(z,\rho) = \Theta(z-d)\Theta(h_2+d-z)\Theta(h_1+d-z-\rho\tan(\alpha)) \end{cases}$$

Here Θ represents the Heavyside function. The third, fourth and fifth terms in the expression of the Hamiltonian describe the diamagnetic, the orbital Zeeman and spin splitting effects respectively.

Given that we modelled our QD by a truncated cone cylindrically symmetric along the growth direction (axis z), we can then write the wave function in the following way: $\Psi_{n,\sigma}(\overrightarrow{r}) = e^{in\theta}\phi_{n,\sigma}(\rho,z)$; and $\sigma = \pm\frac{1}{2}$ is the single particle spin projection of the operator $\overrightarrow{\sigma}$. The introduction of the quantum number $n = 0, \pm1, \pm2...$ gives a natural way to label the wavefunctions (they will be denoted as $|S_i,\sigma\rangle$, $\left|P_i^{\pm},\sigma\right\rangle$, $\left|D_i^{\pm},\sigma\right\rangle$, ... in the rest of the paper, respectively $(i = 1, 2, 3, ...)$). To calculate the electron (hole) eigen energies and eigen states, we use an exact numerical diagonalization on a Fourier Bessel basis over a large cylindric domain. Hence we ex-

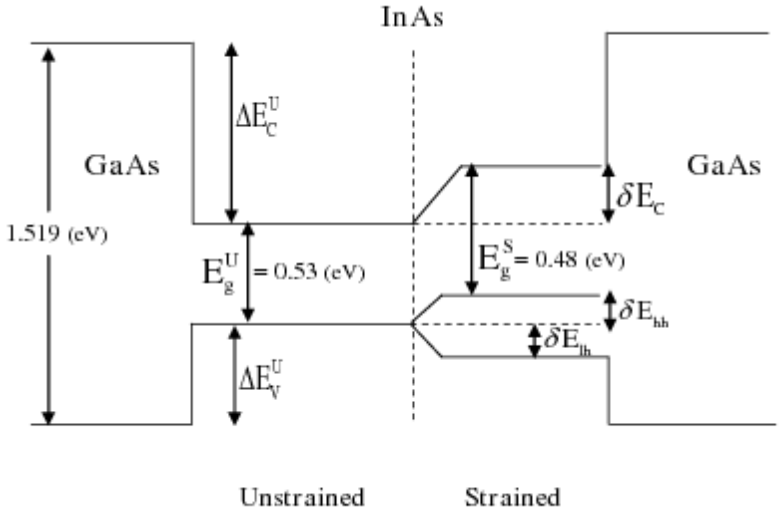

FIG. 4: Band structure model for InAs/GaAs QD.

press the (unknown) function that corresponds to the single particle eigen state $|\Psi_{n,\sigma}\rangle$ as a linear combination of a certain number $i_{\max} \times j_{\max}$ of lineary independent functions $\left|\Phi_{n_{ij},\sigma}\right\rangle$, then we write :

$$\left|\Psi_{n_{ij},\sigma}\right\rangle = \sum_{i,j}^{i_{\max},j_{\max}} c_{ij}^{n,\sigma} \left|\Phi_{n_{ij},\sigma}\right\rangle$$

where $\Phi_{nij}\left(r_{e(h)}\right) = \alpha_i^n e^{in\theta} J_n\left(\frac{\lambda_i^n}{R}\rho_e\right)\sin\left(\frac{\pi j}{Z}z\right)$. In our notations Z and R are respectively the height and the radius of large cylinder. λ_i^n is the ith root of the n-order Bessel function J_n; c_{ij}^n are basis coefficients and α_i^n are the normalization constants. Thus, the whole problem of finding the exact energy eigenvalues of the stationary Schrödinger equation is reduced to the numerical diagonalization of the resulting Hamiltonian matrix.

B. Results

1. *Strain effect*

Using the forty **k.p** theoretical model we performed, we calculated the strain induced by the self assembled growth of InAs/GaAs QDs, and we simulated the elastic energy with a linear elasticity model. The potential profile is obtained by computing the band structure for a periodic lattice with the geometry of the local strained unit cell. In Figure 4 the band structure of our

model is schematically illustrated, and the CB and VB edges of each unit cell along the z growth direction are shown. The VB edge of unstrained InAs (denoted by the subscript U) is set to be zero as reference energy. It is clearly shown that the strain effects are significant on both CBs and VBs. The CB edge in the strained dot is shifted up from 0.697 eV (un-strained InAs conduction band edge) to 0.951 eV, while the VB edge splits to two branches, the HH and LH bands separated the amount $\delta E_{hh} + \delta E_{\ell h} = 0.5$ eV, where δE_{hh} and $\delta E_{\ell h}$ are the corresponding HH and LH induced-strain shifts with respect to the unstrained structure. Otherwise, if we could some how turn off the strain, the holes would be confined by a well that is only 0.288 eV deep. This large splitting of the subbands of LH and HH in the VB reduces considerably the mixing of states from these two subbands. Thus, we restrict ourselves to the study of HH. Our results, and those of others [21–23] revealed that due to the presence of the strain, the band structure of SCs is generally altered, which changes the lattice constant and reduces the symmetry of the crystal. It modifies also energy gaps, removes degeneracy, and modifies the charge carrier confinement potentials. Stoleru et *al* [24] has also indicated that the magnitudes of the strain components depend on the geometries of the dots. This is as it should be for both qualitative and quantitative reasons. It was found for example, that the biaxial strain is very sensitive to the QD shape truncation. Lee et *al* [22] has investigated the effect of the wetting layers on the strain and electronic structure of InAs self-assembled QDs grown on GaAs, with the atomistic valence-force-field model and empirical tight binding model. They found that the effect of the wetting layer on the wave function is qualitatively different for the weakly confined electron state and the strongly confined hole state. More recently, considering a semi-ellipsoidal shaped QD, Filikhin et *al* [25] have presented an effective approach for describing the electronic structure of InAs/GaAs QDs assuming that the total effect of the inter-band interactions, strain and piezoelectricity can be taken into account by an effective potential. Hence, it turns out that if one wants to calculate the single particle energies to the accuracy now required by experiment, the details of the physical structure and most importantly, the strain within each self assembled QD must be included in the calculation. The strain effects obtained here are used next as input parameters to calculate the electron and hole energy dependence as function of the QD size and the applied external magnetic field.

2. ***Size variation***

The results of the effect of the size variation on the electron and hole energy spectrum dependence are presented in this section. We have numerically solved the single particle Hamiltonians using a matrix diagonalization approach. Such technique has proved it self to be a workable and reliable technique [26–29]. The accuracy of the numerical results was well controlled through the increasing of the truncated (finite) basis set dimensionality. Hence we can reach a very good convergence criterion and get the exact numerical solution of the energy eigenvalue problem (ground

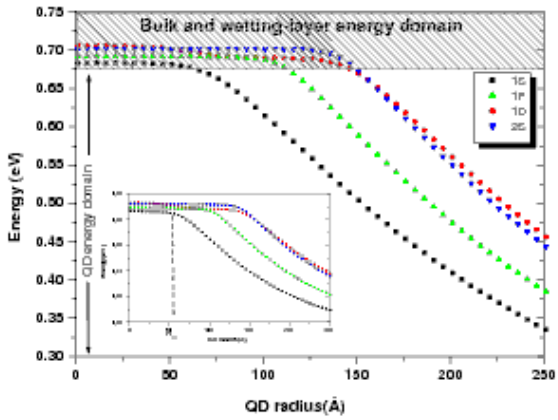

FIG. 5: Variation of the electron energy as a function of QD radius without considering the structure strain. The inset shows the variation of the hole energy as a function of the QD radius without the consideration of the lattice mismatch induced strain.

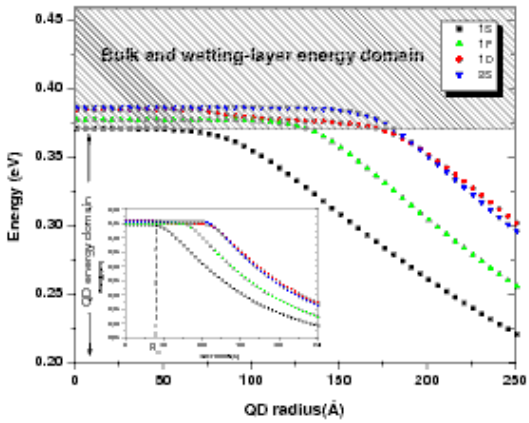

FIG. 6: Variation of the electron energy versus the QD radius in strained InAs/GaAs QD. The inset shows the variation of the hole energy versus the QD radius, considering the structure strain.

state and excited states). In Figure 5, we plotted the electron and hole (in the inset) energy variation versus of the QD radius. It is found that the QD displays discrete levels for energy less than 680 meV for the electrons, and 265 meV for the holes. In the energy domain higher than this value, the electron and hole states are localised in the wetting layer and bulk forming a continuum, where the energy levels are too close to each other. Therefore, the energy spectrum of an electron or a hole confined in a self assembled QD, can be at a good approximation described as truncated spectrum of a two dimensional parabolic well. Such result was confirmed by Jacak et *al* [30]. Considering the strain effect, we plotted in Figure 6 the electron and hole energy dependences versus the dot radius. We can notice that although the charge carriers display

similar energy dependence behaviour compared to the unstrained case, the energy values have changed significantly due to the compressive strain. Consider for example a 100 Å dot radius, the electron energy in this dot, neglecting the strain, is about 615 meV, whereas considering the strain, for the same dot size, the electron energy is equal to 345 meV, which represents almost the half of unstrained electron energy value. However, considering the same 100 Å QD radius for the holes, the energy has shifted up from 210 meV to 315 meV due to the strain. This could be understood because of the HH value band offset that became larger than the unstrained one ΔE_V^U, consequently the holes are then trapped in a deeper quantum well. Whereas, the situation is different for the electrons since the band-offset that corresponds to the strained stucture is reduced by a δE_C energy value compared to that of the unstrained structure ΔE_C^U. Moreover, another interesting results is found for both electrons and holes which is in fact a consequence of the last result. It concerns the particular QD radius from which the localised states appear in the QD. Indeed, from the hole energy spectrum, one can notice that the ground bound state appears, in unstrained QD, for radii larger than $R_D = 58$ Å, while in presence of strain, the critical radius R_D is reduced to 40 Å, as shown on figures 5 and 6. Hence due to the presence of the strain, the hole enegy states in the dot are squeezed. Now concerning the electron energy spectrum, this particular R_D value has rather increased from 60 Å to 70 Å when taking into account the structure strain. In Figure 7 it is shown 3D plots of the electron energy variation as a function of the QD radius and height, for both unstrained and strained structures. The results revealed that for the two situations the electron energy is very sensitive to the quantum height variation. As we pointed out in the first section of this work, Campbell-Ricketts [11] et *al* have recently emphasized the very important role of the dot height in determining optical properties in InAs/GaAs QDs.

3. ***Magnetic field dependence***

We investigated the magnetic field effect on the strained InAs/GaAs QDs, considering a fixed dot size that correspounds to a QD radius R equal to 100 Å. Figure 8 illustrates the lowest part of the energy spectrum of electrons (a), and holes (b) as a function of the magnetic field B. Because of the large inter-level spacing, typical of self assembled QDs, the behaviour with magnetic field is relatively simple. Roy et *al* in Ref.31 have already pointed out such behaviour for $In_xGa_{1-x}As$ dots using also a matrix diagonalization calculation approach. We can easily notice that the magnetic field shows the usual evolution from the quadratic diamagnetic shift at low magnetic fields to the formation of Landau levels in a regime of linear dependence on B. It is important to notice also that upon the inclusion of the Zeeman term added to the spin splitting, all the doublets are split so that all the degeneracy is completely lifted.

Because of the small values of the gyromagnetic ratio g for SC QDs compared to bulk SCs, the

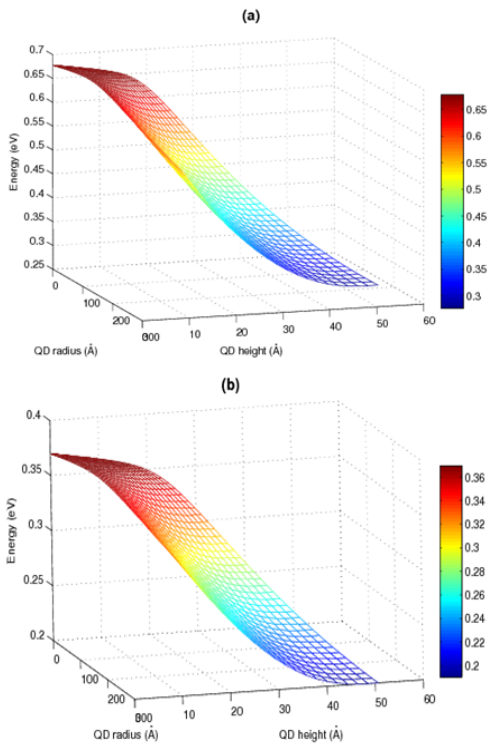

FIG. 7: (a) Simulated dependence of the electron energy on QD radius and height, without considering the strain. (b) Simulated dependence of the electron energy on QD radius and height in Strained InAs/GaAs QDs.

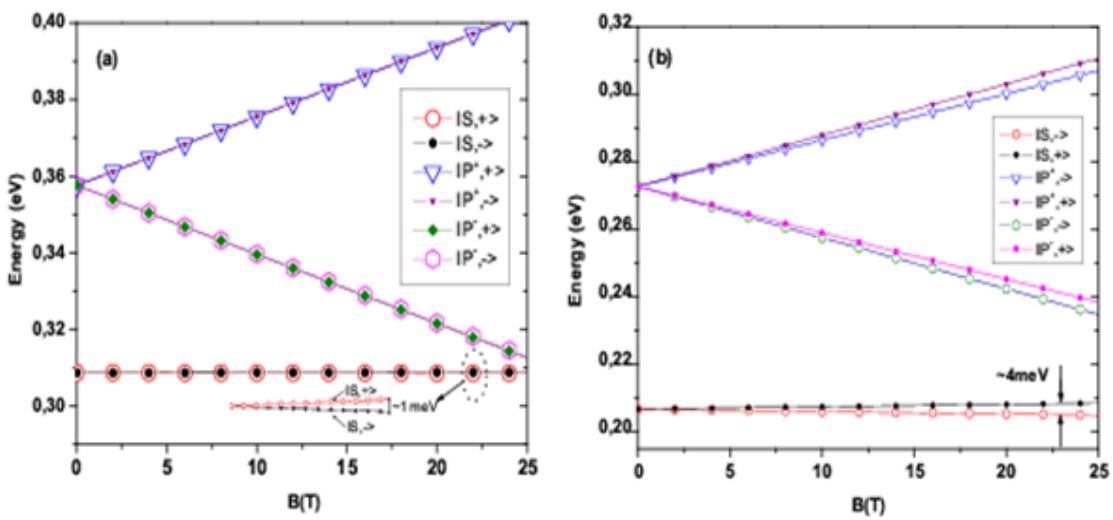

FIG. 8: (a) Magnetic field dependence of the first electron energy states in strained InAs/GaAs QDs. In our calculations we have taken $g_e = 0.18$. (b) Magnetic field dependence of the first hole energy states in strained InAs/GaAs QDs. In our calculations we have taken $g_h = 2.50$.

spin splitting between the spin up and spin down electron and hole states is relatively small. For example, for the $|1S,+\rangle$ and $|1S,-\rangle$ electron levels, the splitting does not exceed 1 meV, however for the hole, the situation is a little bit defferent since the splitting betwen the $|1S,+\rangle$ and $|1S,-\rangle$ states is about 4 meV. This basically comes from the fact that the hole Landé factor g is about thirteen times larger then the electron one. We note that in our work we are interested basically on the effect of magnetic field on the orbital part of the wave function calculated by using a numerical matrix diagonalization approach, therefore for reason of simplicity we have chosen to take the electron and hole Landé factors from the experimental result given by Testelin *et al* [19, 20]. However, we note that recent interesting studies have been performed to investigate the dependence of the effective g Landé factor on the size, strain and magnetic field [32–34]. In our results the use of high magnetic fields could be of particular importance and in tune with recent works performed on quantum dots. For instance, Nuytten et *al* [35] have studied the temperature dependence of the photoluminescence of self-assembled InAs/GaAs QDs in high magnetic fields, they found that a strong magnetic field increases the energy gap between the states in the QDs and the states of the surrounding bulk GaAs material. It turned out also that when applying a magnetic field, the energy levels of the GaAs barrier material are substantially raised, while the increase of the QD levels is rather moderate. Consequently, a strong magnetic field enhances the temperature stability of the system by counteracting the escape of carriers from the dots into the surrounding barrier material. Similar experimental results given by Larsson et *al* [36] have pointed out the enhancement of the photoluminescence intensity observed at temperatures above 100 K using a significant magnetic field.

iven the additional confinement effect that produces the magnetic field on the charge carriers, we expect the influence of the magnetic field on energy levels of the QDs to be strongly dependent on the degree of confinement present in the dots. Hence the magnetic field effect on the electron and hole energy spectra would be more pronounced for relatively large dots that have a weaker confinement potential, resulting in a stronger dependence on the magnetic field.

It should be noted that there has been a large amount of interest in the InAs/GaAs nanostructures, mainly due to the promising potential for applications. In the theoretical previous works, authors such as Bimberg *et al*, Zunger *et al* have used basically the 8-band **k.p** theoretical model to compute the charge carrier confinement energies as well as the magnetic field dependence. In our work we have performed a more sophisticated 40-band model which provides more accurate description of bulk SC band structure. Added to the strain calculation consideration, our numerical model based on the reliable matrix diagonalization technique is able to simulate accurately the diffrent parameters used in the calculation of the quantum dot charge carrier energies. In our work we have chosen a truncated cone shaped quantum dot, since till now experimental results indicate that these structures can have several shapes depending on the manufacturing methodology. Nevertheless, even if the methodology is the same, the experimental results demonstrate that the geometry of the quantum dot remain not precise, and depend on

different physical parameters [37].

IV. CONCLUSION

Using an accurate 40-band **k.p** and Bir-Pikus Hamiltonian model, we simulated first the strained InAs band diagram. We extracted the QD material parameters that we used to calculate the electron and hole energy dependences as a function of the dot size and an external applied magnetic field. We considered thereafter the strain induced by the QD and susbstrate material mismatch on the quantum dot charge carrier energy. Our results revealed that due to the strain, the energy band diagram is clearly modified, and the energy degeneracy of the hole states is lifted. Consequently the electron energy spectrum changed considerably. It was found also that the magnetic field creates out an additional confinement on the charge carriers that affects the electron and hole states. Finally, although in experiments all listed effects contribute together and only a combined effect is observed, theoretical predictions about the signs and the magnitude of the shape, size, strain, and magnetic field effects are obviously useful to chose an external perturbation to modify and control the electronic and optical properties of QDs.

V. ACKNOWLEDGMENTS

This work was carried out under the joint Tuniso-French research project (CMCU, 09G1307). One of the authors (K.S) is particularly grateful to the Kuwait Foundation for the Advancement of Sciences (KFAS), to its Director Dr. Khalid S. Al-Muhailan, and also to the Condensed Matter and Statistical Physics group at the Abdus Salam International Centre for theoretical Physics (ICTP) for the partial financial support, and for providing the necessary facilities and literature for the present work.

References

[1] K. Sellami and S. Jaziri, phys. Stat. sol. (c) **3**, 3347 (2006).

[2] Nano-Optoelectronics Concepts, Physics and Devices, edited by M. Grundmann (Springer-Verlag, Berlin, 2002).

[3] S. Raymond, S. Studenikin, A. Sachrajda, Z. Wasilewski, S. J. Cheng, P. Hawrylak, M. Potemski, G. Ortner, and M. Bayer, Phys. Rev. Lett. **92**, 187402 (2004).

[4] K. Sellami, I. Zgaren, and S. Jaziri, Sensor. Lett. **7**, 962 (2009).

[5] M. Henini, 2nd CEPHONA Workshop on Microscopic characterisation of materials and Structures for photonics, Warsaw, (2004).

[6] M. Henini, Handbook of Self Assembled Semiconductor Nanostructures for Novel Devices in Photonics and Electronics (Elsevier Science, Amsterdam, 2008).

[7] J. H. Lee, Zh. M. Wang, B. L. Liang, K. A. Sablon, N. W. Strom and G. J. Salamo, Semicond. Sci. Technol. **21**, 1547 (2006).

[8] Z. M. Wang, Self-Assembled Quantum Dots (Springer-Verlag, New York, 2008)

[9] D. Reuter, P. Kailuweit, A. D. Wieck, U. Zeitler, O. Wibbelhoff, C. Meier, A. Lorke, and J. C. Maan, Phys. Rev. Lett. **94**, 026808 (2005).

[10] R. J. Young, R. M. Stevenson, A. J. Shields, P. Atkinson, K. Cooper, D. A. Ritchie, K. M. Groom, A. I. Tartakovskii, M.S. Skolnick, Phys. Rev. B **72**, 113305 (2005).

[11] T. E. J. Campbell-Ricketts, N. A. J. M. Kleemans, R. Nötzel, A. Yu. Silov, and P. M. Koenraad, Appl. Phys. Lett. **96**, 033102 (2010).

[12] C. Y. Ngo, S. F. Yoon, W. Fan, and S. J. Chua, Opt. Quantum. Electron **38**, 981 (2006).

[13] K. Sellami and S. Jaziri, Superlattices Microstruct. **37**, 43 (2005).

[14] T. Nuytten, M. Hayne, M. Henini, Phys. Rev. B **77**, 115348 (2008).

[15] I. Saidi, S. Ben Radhia, and K. Boujdaria, J. Appl. Phys. **107**, 043701 (2010).

[16] G. L. Bir and G. E. Pikus, Symmetry and Strain-Induced Effects in Semiconductors (Wiley, New York, 1974).

[17] See, for example, Thomas B. Bahder, Phys. Rev. B **41**, 11992 (1990).

[18] S. Richard, F. Aniel, and G. Fishman. J. Appl. Phys. **94**, 1795 (2003).

[19] E. Aubry, C. Testelin, F. Bernardot, M. Chamarro, and A. Lemaître, Appl. Phys. Lett. **90**, 242113 (2007).

[20] C. Testelin, E. Aubry, B. Eble, F. Bernardot, M. Chamarro and A. Lemaître, Physica E **40**, 2072 (2008).

[21] H. Jiang and J. Singh, Phys. Rev. B **56**, 4696 (1997).

[22] S. Lee, O. L. Lazarenkova, P. Von Allmen, F. Oyafuso, and G. Klimeck, Phys. Rev. B **70**, 125307 (2004).

[23] S. Adhikary, N. Halder, S. Chakrabarti, S. Majumdar, S.K. Ray, M. Herrera, M. Bonds, N.D. Browning, J. Cryst. Growth. **312**, 724 (2010).

[24] V.G. Stoleru, D. Pal, E. Towe, Physica E **15**, 131 (2002).

[25] I. Filikhin, V. M. Suslov, M. Wu, B. Vlahovic, Physica E **41**, 1358 (2009).

[26] J.-Y. Marzin, G. Bastard, Solid State Commun. **92**, 437 (1994) .

[27] Ph. Lelong, G. Bastard, Solid State Commun. **98**, 819 (1996).

[28] P. Harrison, Quantum Wells, Wires and Dots: Theoretical and Computational Physics of Semiconductor Nanostructures (Wiley Interscience, New York, 2005).

[29] Quantum Dots: Research, Technology and Applications, edited by R. W. Knoss (Nova Science, New York, 2009).

[30] L. Jacak, P. Hawrylak, and A. Wojs, Quantum Dots (Springer, Berlin, 1998).

[31] Mervyn Roy and P. Maksyn. Phys. Rev. B **68**, 235308 (2003).

[32] T. Nakaoka, T. Saito, J. Tatebayashi, and Y. Arakawa, Phys. Rev. B **70**, 235337 (2004).

[33] Craig E. Pryor and M. Flatt, Phys. Rev. Lett. **96**, 026804 (2006).

[34] T. Andlauer, R. Morschl, and P. Vogl, Phys. Rev. B. **78**, 075317 (2008).

[35] T. Nuytten, M. Hayne, M, Henini, V. V. Moshchalkov. Microelectronics Journal **40**, 486 (2009).

[36] M. Larsson, E. S. Moskalenko, L. A. Larsson and P. O. Holtz. Phys. Rev. B **74**, 245312 (2006).

[37] C. Tablero, J. Appl. Phys **106**, 074306 (2009).